Static Voltage Stability Analysis of Distribution Systems Based on Network-Load Admittance Ratio

Yue Song, *Member, IEEE*, David J. Hill, *Life Fellow, IEEE*, and Tao Liu, *Member, IEEE*

***Abstract*—It is well known that a single (constant power) load infinite-bus system reaches a static voltage stability limit point, or equivalently, a singularity point of the power flow Jacobian, at the unity line-load admittance ratio, i.e., the equivalent admittance of the load has the same modulus as the transmission line admittance. In this paper, we rigorously extend this result to generic distribution systems with distributed generators (DGs). We introduce a new concept called the network-load admittance ratio that is in terms of the parameters of power network, loads, and DGs. This concept is a generalization of the line-load admittance ratio that characterizes the loading status of a distribution system with the effects of DGs included. We prove that the power flow Jacobian is singular if and only if the network-load admittance ratio is unity, which provides new insights into the mechanism of voltage stability. In addition, we establish a new voltage stability index by using the network-load admittance ratio. Numerical simulations on several IEEE test systems show that the index has good linearity with load increase and estimates voltage stability margin with high precision. The index also reflects the impact of DG penetration level and control mode on voltage stability. The obtained results can be extended to ZIP load models, unbalanced three-phase networks, and mesh networks with slight modifications.**

***Index Terms*—Distribution network, power flow Jacobian, singularity point, voltage stability, voltage stability index.**

I. Introduction

THE static properties of power flow equations, e.g., the existence and sensitivity behaviour of power flow solution for a given load and generation pattern, are of major concern in maintaining long-term voltage stability, which is important in power system planning and operation [1], [2]. In this paper we focus on the voltage stability problem under the long-term time frame where static models apply, and henceforth use the term "voltage stability" for simplicity. In the early literature, voltage stability problems in high-voltage transmission systems used to receive more attention than those in distribution systems. Thanks to renewable energy technology, the growing penetration of distributed generators (DGs) leads to a transition of distribution systems from passive users to active participants in system dispatch. On the other hand, the DG integration significantly changes the features of power flows and voltage profiles, which pose new challenges. Voltage stability problems in distribution systems are now getting serious and drawing increasing concern [3]–[5].

The singularity point of power flow Jacobian, which indicates a critical state for the existence of power flow solution, is a class of static voltage stability limit of most interest to power engineers. The traditional Newton-Raphson method fails to converge when the power flow Jacobian is close to singularity, which adds difficulties to calculating the exact singularity point. Many advanced tools have been developed to address this problem, such as Iwamoto's method [6], continuation power flow (CPF) [7], [8] and holomorphic embedding method [9], to name just a few. In [10], [11], a general optimization model is proposed that provides a unified computation framework for power flow Jacobian singularity as well as other kinds of secure operation limit points. Also, some useful stability indices have been designed based on eigen-decomposition of the power flow Jacobian at the singularity point [12], [13]. The local geometry of the stability limit surface can be characterized by the eigenvector with respect to the zero eigenvalue of power flow Jacobian [14].

In addition to those efforts on numerical issues, researchers have developed some voltage stability criteria. A well-known one is for the single-(constant power) load infinite-bus system. It says that the power flow Jacobian reaches a singularity point at the unity line-load admittance ratio, i.e., the equivalent admittance/impedance of the load has the same modulus as that of the transmission line [1]. An extension of this result to multi-load systems is reported in [15], which only holds under some restrictive requirements on the network topology and R/X ratio of lines. Another way of extension is to reduce the original system to a two-bus system by using Thevenin equivalent, so that the criterion of the unity line-load admittance ratio can be applied (e.g., see [16]–[20]). Branch equivalents are also adopted in the literature for network reduction [21]–[23]. The L-index is proposed in [24] by a derivation similar in spirit to the criterion of the unity line-load admittance ratio. Overall, these results are based on approximations and/or heuristics rather than rigorous theorems.

Manuscript received June 7, 2018; revised October 10, 2018; accepted December 1, 2018. Date of publication December 13, 2018; date of current version April 17, 2019. This work was supported in part by the Hong Kong Ph.D. Fellowship Scheme, and in part by the Research Grants Council of the Hong Kong Special Administrative Region through the General Research Fund under Project 17208817 and through the Theme-Based Research Scheme under Project T23-701/14-N. Paper no. TPWRS-00879-2018. *(Corresponding author: Yue Song.)*

Y. Song and T. Liu are with the Department of Electrical and Electronic Engineering, The University of Hong Kong, Hong Kong (e-mail: yuesong@eee.hku.hk; taoliu@eee.hku.hk).

D. J. Hill is with the Department of Electrical and Electronic Engineering, The University of Hong Kong, Hong Kong, and also with the School of Electrical and Information Engineering, The University of Sydney, Sydney, NSW 2006, Australia (e-mail: dhill@eee.hku.hk).

Color versions of one or more of the figures in this paper are available online at http://ieeexplore.ieee.org.

Digital Object Identifier 10.1109/TPWRS.2018.2886636

For generic power systems, the rigorous results mainly refer to sufficient or necessary conditions for voltage stability. In [25], [26], sufficient conditions for the solvability of reactive power-voltage equations are established by exploiting the decoupling between active power and reactive power in transmission systems. The necessary condition proposed in [27] shows that a path from the source to sink formed by the transmission lines hitting their transfer stability limits will appear before the system reaches a voltage stability limit point. Particularly, some unique properties held by distribution systems have inspired specific but insightful results. The radial structure of distribution networks leads to a unique power flow solution with feasible voltage magnitudes (see [28] and the extension to three-phase radial networks [29]). In addition, power flow equations of distribution systems can be formulated into a neat form due to the absence of PV buses. This property is leveraged to obtain explicit conditions for the existence of power flow solution (e.g., see [3], [4], [30]). However, there is still a lack of necessary and sufficient condition that interprets voltage stability of generic distribution systems in a concise way as the criterion of the unity line-load admittance ratio.

In this paper, we generalize the criterion of the unity line-load admittance ratio to generic distribution systems. We define a new concept namely the "network-load admittance ratio" that characterizes the system loading status. The network-load admittance ratio is in terms of the power network admittance matrix and the equivalent admittances of net loads, and the effects of constant-power and constant-current DGs are taken into consideration. A necessary and sufficient condition for voltage stability is established, which shows that the power flow Jacobian singularity is equivalent to the unity network-load admittance ratio. This result concisely interprets the role of power network structure, loads and DGs in voltage stability. It includes the criterion of the unity line-load admittance ratio as a special case for the single-load infinite-bus system. Moreover, a new voltage stability index is proposed based on this result. The new index is highly linear with load increase, and thus can better estimate voltage stability margin. It can also be used as an indicator of the impact of the DG penetration level and control mode on voltage stability. These results can be easily extended to ZIP loads, unbalanced three-phase networks and mesh networks.

The rest of the paper is organized as follows. The power flow model of distribution systems with DGs is formulated in Section II. The criterion of the unity line-load admittance ratio is briefly reviewed, and the new theorems and voltage stability index are established in Section III. Section IV discusses some extensions of the obtained results. Section V gives numerical simulations on several IEEE test systems to verify the results. Section VI concludes the paper.

Notations: Let $\mathbb{C}$ denote the set of complex numbers and $\mathbb{R}$ the set of real numbers. Let $\boldsymbol{A} \in \mathbb{C}^{p\times q}$ be a matrix, $\overline{\boldsymbol{A}} \in \mathbb{C}^{p\times q}$ denotes the entry-wise complex conjugate of $\boldsymbol{A}$. For simplicity, a vector $\boldsymbol{x} = [x_1, x_2, ..., x_p]^T \in \mathbb{C}^p$ is denoted as $\boldsymbol{x} = [x_i] \in \mathbb{C}^p$, and a diagonal matrix $\boldsymbol{A} = \text{diag}\{a_1, a_2, ..., a_p\} \in \mathbb{C}^{p\times p}$ is denoted as $\boldsymbol{A} = \text{diag}\{a_i\} \in \mathbb{C}^{p\times p}$. The notation $|x|$ denotes the modulus of $x \in \mathbb{C}$, and $\text{Re}\{x\}$ and $\text{Im}\{x\}$ denote the real part and imaginary part of $x \in \mathbb{C}$, respectively. $\boldsymbol{I}_p \in \mathbb{R}^{p\times p}$ denotes the identity matrix. We a bit abuse the notation j, the italic j denotes a numbering index, and the upright j denotes the square root of -1. In addition, we will interchangeably use $a + \text{j}b$ and $r\angle\phi$ to represent a complex number where $a = r\cos\phi$ and $b = r\sin\phi$.

II. Power Flow Equations of Distribution Systems

Consider a distribution system with one slack bus that represents the substation and n PQ buses that may connect loads and DGs. Assume the system is three-phase balanced so that the analysis is carried out on the per-phase equivalent circuit. The admittance matrix of the distribution network is denoted as $\boldsymbol{Y} = \boldsymbol{G} + \text{j}\boldsymbol{B} \in \mathbb{C}^{(n+1)\times(n+1)}$, where $\boldsymbol{G}, \boldsymbol{B}$ are the real part and imaginary part, respectively. We number the PQ buses from bus 1 to bus n, and the slack bus is bus n+1. For each bus i, denote $\theta_i, V_i \in \mathbb{R}$ as its phase angle and voltage magnitude. The slack bus has a fixed phase angle $\theta_{n+1} = 0$ and voltage magnitude $V_{n+1} = V_{n+1}^0$. The voltage of PQ bus i, $i = 1, ..., n$, is described by the power flow equations below

$$\begin{aligned} 0 = f_i &= V_i^2 G_{ii} + \sum_{j\in\mathcal{N}_i} V_i V_j |Y_{ij}| \sin(\theta_{ij} - \varphi_{ij}) \\ &\quad - P_{Gi} + P_{Li} \\ 0 = h_i &= -V_i^2 B_{ii} - \sum_{j\in\mathcal{N}_i} V_i V_j |Y_{ij}| \cos(\theta_{ij} - \varphi_{ij}) \\ &\quad - Q_{Gi} + Q_{Li} \end{aligned} \tag{1}$$

where θ_{ij} is defined as $\theta_{ij} = \theta_i - \theta_j$; P_{Li}, P_{Gi} denote the active power load and active power generation of the DG at bus i, respectively; Q_{Li}, Q_{Gi} denote the reactive power load and reactive power generation of the DG at bus i, respectively; $\mathcal{N}_i$ denotes the set of neighbouring buses of bus i, the notation $j \in \mathcal{N}_i$ means bus i and bus j are connected by a line; Y_{ij}, G_{ij} and B_{ij} are the (i, j) entry of the matrices $\boldsymbol{Y}$, $\boldsymbol{G}$ and $\boldsymbol{B}$, respectively; the term $\varphi_{ij} = -\tan^{-1}\frac{G_{ij}}{B_{ij}}$ is the phase shift caused by line loss, and we set $\varphi_{ij} = 0$ in case that $Y_{ij} = 0$, i.e., bus i and bus j are not connected by a line. We consider two main DG control modes in distribution systems—constant-power (CP) mode and constant-current (CC) mode. The active and reactive power generation of a CP-DG are $P_{Gi}^{\text{CP}}, Q_{Gi}^{\text{CP}}$, and those of a CC-DG are $I_{pi}^{\text{CC}} V_i, I_{qi}^{\text{CC}} V_i$, where $P_{Gi}^{\text{CP}}, Q_{Gi}^{\text{CP}}, I_{pi}^{\text{CC}}, I_{qi}^{\text{CC}}$ are constants [31]. Then, the generation at bus i can be expressed by the following compact form

$$\begin{aligned} P_{Gi} &= P_{Gi}^{\text{CP}} + I_{pi}^{\text{CC}} V_i \\ Q_{Gi} &= Q_{Gi}^{\text{CP}} + I_{qi}^{\text{CC}} V_i \end{aligned} \tag{2}$$

where $P_{Gi}^{\text{CP}} = Q_{Gi}^{\text{CP}} = 0$ if bus i connects a CC-DG and $I_{pi}^{\text{CC}} = I_{qi}^{\text{CC}} = 0$ if bus i connects a CP-DG. In addition, we adopt the constant-power load model first. It will be shown in Section IV that the obtained results can be extended to ZIP loads, and furthermore, to unbalanced three-phase distribution systems.

Denote $(\boldsymbol{\theta}, \boldsymbol{V})$ as the power flow solution to the given $\theta_{n+1}^0, V_{n+1}^0$ and $P_{Gi}^{\text{CP}}, Q_{Gi}^{\text{CP}}, I_{pi}^{\text{CC}}, I_{qi}^{\text{CC}}, P_{Li}, Q_{Li}$, $i = 1, ..., n$, where $\boldsymbol{\theta} = [\theta_i], \boldsymbol{V} = [V_i] \in \mathbb{R}^n$ are the vectors of PQ bus angles

and voltage magnitudes, respectively. Taking derivative of (1) at the solution $(\boldsymbol{\theta}, \boldsymbol{V})$ gives

$$\begin{bmatrix} \Delta \boldsymbol{f} \\ \Delta \boldsymbol{h} \end{bmatrix} = \begin{bmatrix} \boldsymbol{J}_{P\theta} & \boldsymbol{J}_{PV} \\ \boldsymbol{J}_{Q\theta} & \boldsymbol{J}_{QV} \end{bmatrix} \begin{bmatrix} \Delta \boldsymbol{\theta} \\ \Delta \boldsymbol{V}/\boldsymbol{V} \end{bmatrix} = \boldsymbol{J}_{pf} \begin{bmatrix} \Delta \boldsymbol{\theta} \\ \Delta \boldsymbol{V}/\boldsymbol{V} \end{bmatrix} \quad (3)$$

where the notation "/" means the entry-wise division for two vectors. The matrix $\boldsymbol{J}_{pf} \in \mathbb{R}^{2n\times 2n}$ is the power flow Jacobian. The entries of the sub-matrix $\boldsymbol{J}_{P\theta} \in \mathbb{R}^{n\times n}$, denoted $(\boldsymbol{J}_{P\theta})_{ij} = \frac{\partial f_i}{\partial \theta_j}$, $i, j = 1, ..., n$, take values as:

$$(\boldsymbol{J}_{P\theta})_{ij} = \begin{cases} \sum_{k\in\mathcal{N}_i} V_i V_k |Y_{ik}| \cos(\theta_{ik} - \varphi_{ik}), \ i = j \\ -V_i V_j |Y_{ij}| \cos(\theta_{ij} - \varphi_{ij}), \ i \neq j. \end{cases} \quad (4)$$

The entries of the sub-matrix $\boldsymbol{J}_{PV} \in \mathbb{R}^{n\times n}$, denoted $(\boldsymbol{J}_{PV})_{ij} = V_j \frac{\partial f_i}{\partial V_j}$, take values as:

$$(\boldsymbol{J}_{PV})_{ij} = \begin{cases} \sum_{k\in\mathcal{N}_i} V_i V_k |Y_{ik}| \sin(\theta_{ik} - \varphi_{ik}) \\ +2V_i^2 G_{ii} - I_{pi}^{\mathrm{CC}} V_i, \ i = j \\ V_i V_j |Y_{ij}| \sin(\theta_{ij} - \varphi_{ij}), \ i \neq j. \end{cases} \quad (5)$$

The entries of the sub-matrix $\boldsymbol{J}_{Q\theta} \in \mathbb{R}^{n\times n}$, denoted $(\boldsymbol{J}_{Q\theta})_{ij} = \frac{\partial h_i}{\partial \theta_j}$, take values as:

$$(\boldsymbol{J}_{Q\theta})_{ij} = \begin{cases} \sum_{k\in\mathcal{N}_i} V_i V_k |Y_{ik}| \sin(\theta_{ik} - \varphi_{ik}), \ i = j \\ -V_i V_j |Y_{ij}| \sin(\theta_{ij} - \varphi_{ij}), \ i \neq j. \end{cases} \quad (6)$$

The entries of the sub-matrix $\boldsymbol{J}_{QV} \in \mathbb{R}^{n\times n}$, denoted $(\boldsymbol{J}_{QV})_{ij} = V_j \frac{\partial h_i}{\partial V_j}$, take values as:

$$(\boldsymbol{J}_{QV})_{ij} = \begin{cases} -\sum_{k\in\mathcal{N}_i} V_i V_k |Y_{ik}| \cos(\theta_{ik} - \varphi_{ik}) \\ -2V_i^2 B_{ii} - I_{qi}^{\mathrm{CC}} V_i, \ i = j \\ -V_i V_j |Y_{ij}| \cos(\theta_{ij} - \varphi_{ij}), \ i \neq j. \end{cases} \quad (7)$$

The singularity point of the power flow Jacobian is regarded as a voltage stability limit point [1]. The singularity has direct physical meanings. It implies that the power flow Jacobian is non-invertible and there exist infinite sensitivities in the solution to parameter perturbations (e.g., dV/dQ sensitivities in case of constant-power loads). In addition, the singularity point refers to the saddle node bifurcation of the system where the high-voltage and low-voltage solutions coalesce and disappear [2]. Also note that the power flow Jacobian $\boldsymbol{J}_{pf}$ in (3) is slightly different from the conventional definition. The conventional power flow Jacobian, say $\boldsymbol{J}_{pf}^{\mathrm{conv}}$, is defined by

$$\boldsymbol{J}_{pf}^{\mathrm{conv}} = \begin{bmatrix} \frac{\partial \boldsymbol{f}}{\partial \boldsymbol{\theta}} & \frac{\partial \boldsymbol{f}}{\partial \boldsymbol{V}} \\ \frac{\partial \boldsymbol{h}}{\partial \boldsymbol{\theta}} & \frac{\partial \boldsymbol{h}}{\partial \boldsymbol{V}} \end{bmatrix} = \boldsymbol{J}_{pf} \begin{bmatrix} \boldsymbol{I}_n & \boldsymbol{0} \\ \boldsymbol{0} & \boldsymbol{D}_V^{-1} \end{bmatrix} \quad (8)$$

where $\boldsymbol{D}_V = \mathrm{diag}\{V_i\} \in \mathbb{R}^{n\times n}$. Equation (8) implies that $\boldsymbol{J}_{pf}$ and $\boldsymbol{J}_{pf}^{\mathrm{conv}}$ have the same singularity points and hence play the same role in indicating voltage stability limit. In the following, we will focus on the singularity condition for the power flow Jacobian $\boldsymbol{J}_{pf}$ defined by (3) as the expression brings much convenience to our analysis.

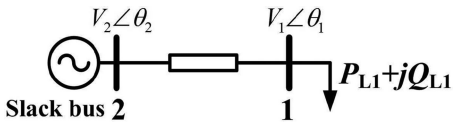

Fig. 1. A single-load infinite-bus system.

III. Power Flow Jacobian Singularity and Network-Load Admittance Ratio

A. Review of Single-Load Infinite-Bus System

In this section, we will establish a necessary and sufficient condition for power flow Jacobian singularity and a new voltage stability index. Before presenting the main results, let us have a brief review of the existing results for the single-load infinite-bus system in Fig. 1, which is the simplest system for voltage stability study. In this system, the power flow equations of bus 1 are

$$\begin{aligned} 0 = f_1 &= V_1^2 G_{11} + V_1 V_2 |Y_{12}| \sin(\theta_{12} - \varphi_{12}) + P_{L1} \\ 0 = h_1 &= -V_1^2 B_{11} - V_1 V_2 |Y_{12}| \cos(\theta_{12} - \varphi_{12}) + Q_{L1} \end{aligned} \quad (9)$$

so that the power flow Jacobian takes the form

$$\boldsymbol{J}_{pf} = \begin{bmatrix} \frac{\partial f_1}{\partial \theta_1} & \frac{\partial f_1}{\partial V_1} V_1 \\ \frac{\partial h_1}{\partial \theta_1} & \frac{\partial h_1}{\partial V_1} V_1 \end{bmatrix} \quad (10)$$

where

$$\begin{aligned} \frac{\partial f_1}{\partial \theta_1} &= V_1 V_2 |Y_{12}| \cos(\theta_{12} - \varphi_{12}) \\ \frac{\partial f_1}{\partial V_1} V_1 &= V_1 V_2 |Y_{12}| \sin(\theta_{12} - \varphi_{12}) + 2V_1^2 G_{11} \\ \frac{\partial h_1}{\partial \theta_1} &= V_1 V_2 |Y_{12}| \sin(\theta_{12} - \varphi_{12}) \\ \frac{\partial h_1}{\partial V_1} V_1 &= -V_1 V_2 |Y_{12}| \cos(\theta_{12} - \varphi_{12}) - 2V_1^2 B_{11}. \end{aligned} \quad (11)$$

Combining (9) and (11) gives

$$\boldsymbol{J}_{pf} = \begin{bmatrix} Q_{L1} - V_1^2 B_{11} & -P_{L1} + V_1^2 G_{11} \\ -P_{L1} - V_1^2 G_{11} & -Q_{L1} - V_1^2 B_{11} \end{bmatrix}. \quad (12)$$

Since $Y_{11} = -Y_{12}$ in this case, it follows from (12) that the singularity of power flow Jacobian is equivalent to the following condition

$$P_{L1}^2 + Q_{L1}^2 = (G_{11}^2 + B_{11}^2) V_1^4 = |Y_{12}|^2 V_1^4. \quad (13)$$

Denote $Y_{L1}^{\mathrm{eq}} = \frac{P_{L1} - jQ_{L1}}{V_1^2}$ as the equivalent admittance of the constant-power load at bus 1. The power consumed by Y_{L1}^{eq} is $P_{L1} + \mathrm{j}Q_{L1}$. Then (13) can be reformulated into the criterion of the unity line-load admittance ratio below

$$|(Y_{L1}^{\mathrm{eq}})^{-1} Y_{12}| = 1. \quad (14)$$

The line-load admittance ratio $|(Y_{L1}^{\mathrm{eq}})^{-1} Y_{12}|$ indicates the system loading status. Condition (14) implies that the modulus of load admittance matches that of line, i.e., the maximum loadability of the line is reached. Note that in this simple system,

(14) also coincides with the maximum power transfer condition under a given load power factor [1].

As aforementioned, so far the extensions of this criterion are mainly based on heuristic reasoning. In the next subsection, we will make a rigourous extension to generic distribution systems by using a new concept called the network-load admittance ratio.

B. Theoretical Results for Generic Distribution Systems

We first introduce some notations for the convenience of analysis. Denote $S_i = P_i + \mathrm{j}Q_i$ as the complex power injection at bus i where $P_i = P_{Gi} - P_{Li}$ and $Q_i = Q_{Gi} - Q_{Li}$ are the active and reactive power injection at bus i, respectively. Denote $S_{Li} = P_{Li} + \mathrm{j}Q_{Li}$ as the complex power load at bus i, $S_{Gi}^{\mathrm{CP}} = P_{Gi}^{\mathrm{CP}} + \mathrm{j}Q_{Gi}^{\mathrm{CP}}$ as complex power generation of the CP-DG at bus i, and $S_{Gi}^{\mathrm{CC}} = I_{pi}^{\mathrm{CC}}V_i + \mathrm{j}I_{qi}^{\mathrm{CC}}V_i$ as the complex power generation of the CC-DG at bus i. With these notations, we propose the definitions below.

Definition 1: Define $\boldsymbol{Y}_d^{\mathrm{eq}} = \mathrm{diag}\{Y_{di}^{\mathrm{eq}}\} \in \mathbb{C}^{n\times n}$ as the equivalent admittance matrix of net loads with phase shift, where

$$Y_{di}^{\mathrm{eq}} = \frac{\overline{S}_{Li} - \overline{S_{Gi}^{\mathrm{CP}}} - \frac{1}{2}\overline{S_{Gi}^{\mathrm{CC}}}}{V_i^2} \cdot 1\angle 2\theta_i,\ i = 1, ..., n \tag{15}$$

Definition 2: Define the matrix $\boldsymbol{Y}_n \in \mathbb{C}^{n\times n}$ as the admittance matrix of the power network (among PQ buses) with CC-DGs incorporated. The entries of $\boldsymbol{Y}_n$, say $(\boldsymbol{Y}_n)_{ij}$, $i, j = 1, ..., n$, take values as

$$(\boldsymbol{Y}_n)_{ij} = \begin{cases} Y_{ii} + \frac{1}{2}\frac{-\overline{S_{Gi}^{\mathrm{CC}}}}{V_i^2}, & i = j \\ Y_{ij}, & i \neq j. \end{cases} \tag{16}$$

Assume the matrix $\boldsymbol{Y}_d^{\mathrm{eq}}$ is nonsingular, and let $\boldsymbol{Y}_{n/d} = (\boldsymbol{Y}_d^{\mathrm{eq}})^{-1}\boldsymbol{Y}_n \in \mathbb{C}^{n\times n}$ be the matrix in a "network divided by load" manner. Then we have the following concept.

Definition 3: Define $R_{n/d} = \sqrt{\lambda^*}$ as the network-load admittance ratio, where

$$\begin{aligned} \lambda^* = \arg\min_{\lambda_i} |\lambda_i - 1| \\ \text{s.t.} \quad \lambda_i \in \mathrm{spec}\{\boldsymbol{Y}_{n/d}\overline{\boldsymbol{Y}}_{n/d}\} \\ \mathrm{Re}\{\lambda_i\} \geq 0,\ \mathrm{Im}\{\lambda_i\} = 0 \end{aligned} \tag{17}$$

and $\mathrm{spec}\{\cdot\}$ denotes the spectrum of a matrix and $\arg\min$ denotes the argument of the minimum.

In the above definitions, the effects of CP-DGs are entirely equivalent to net loads (see (15)), while the effect of a CC-DG is divided into two parts. Part of the CC-DG generation is equivalent to net load (see (15)), while the other part is equivalent as an additional shunt admittance in the power network (see (16)). Fig. 2 gives an illustration of the equivalents of CP-DGs and CC-DGs in $\boldsymbol{Y}_d^{\mathrm{eq}}$ and $\boldsymbol{Y}_n$. The two-part equivalent of CC-DGs will lead to a neat result that describes the spectrum of power flow Jacobian in terms of $\boldsymbol{Y}_d^{\mathrm{eq}}$ and $\boldsymbol{Y}_n$ (see Lemma 1). It also hints that CC-DGs and CP-DGs have different impacts on voltage stability, which will be discussed later.

The network-load admittance ratio given in Definition 3 is a generalization of the line-load admittance ratio. Clearly, it reduces to the line-load admittance ratio for a single-load

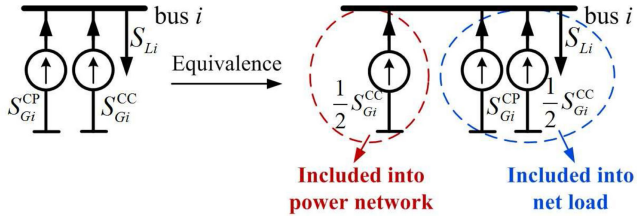

Fig. 2. Illustration of CP-DG and CC-DG equivalents.

infinite-bus system. For generic distribution systems, the network-load admittance ratio can be interpreted as the system loading status with the effect of DGs considered. It should be pointed out that the network-load admittance ratio is different from the line-load admittance ratio of a two-bus system obtained by Thevenin equivalent. The latter one represents a port equivalent looking from a local load, while the former one is an aggregated description of the entire system. In addition, the non-singularity of $\boldsymbol{Y}_d^{\mathrm{eq}}$ adopted in Definition 3 practically holds if there is no tie bus with zero load and generation. Two approaches can be adopted to deal with the situation where this is not the case. One approach is to eliminate the tie buses via Kron reduction [32], but it breaks the original network structure. The other approach preserves the network structure by perturbing $Y_{di}^{\mathrm{eq}} = 0$ as $Y_{di}^{\mathrm{eq}} = \epsilon$, i.e., adding a sufficiently small fictitious load to tie bus i. This approach leads to a non-singular $\boldsymbol{Y}_d^{\mathrm{eq}}$ and large-modulus eigenvalue in the matrix $\boldsymbol{Y}_{n/d}\overline{\boldsymbol{Y}}_{n/d}$. However, it will not impact the network-load admittance ratio, which is only related to the real eigenvalue of $\boldsymbol{Y}_{n/d}\overline{\boldsymbol{Y}}_{n/d}$ that is closest to one. It will be shown in the case study that this approach works properly.

The network-load admittance ratio can be numerically given by $R_{n/d} = \sqrt{\lambda_{\min}(\boldsymbol{Y}_{n/d}\overline{\boldsymbol{Y}}_{n/d} - \boldsymbol{I}_n) + 1}$, where $\lambda_{\min}$ denotes the eigenvalue with the minimum modulus. The reason for this expression is that $\lambda_{\min}(\boldsymbol{Y}_{n/d}\overline{\boldsymbol{Y}}_{n/d} - \boldsymbol{I}_n)$ is usually a real number, which is true in all our tests. Also we point out that $\boldsymbol{Y}_{n/d}\overline{\boldsymbol{Y}}_{n/d} - \boldsymbol{I}_n$ is a sparse matrix due to the property of $\boldsymbol{Y}_{n/d}$. The computational cost of $R_{n/d}$ is relatively low as efficient solvers [33] are available for calculating $\lambda_{\min}(\boldsymbol{Y}_{n/d}\overline{\boldsymbol{Y}}_{n/d} - \boldsymbol{I}_n)$.

With these concepts, we establish the main results below.

Lemma 1: The power flow Jacobian $\boldsymbol{J}_{pf}$ is similar to the matrix

$$\widetilde{\boldsymbol{J}} = \mathrm{j}\cdot\begin{bmatrix} \boldsymbol{V}^c & \boldsymbol{0} \\ \boldsymbol{0} & \overline{\boldsymbol{V}^c} \end{bmatrix}\begin{bmatrix} -\overline{\boldsymbol{Y}}_n & -\overline{\boldsymbol{Y}_d^{\mathrm{eq}}} \\ \boldsymbol{Y}_d^{\mathrm{eq}} & \boldsymbol{Y}_n \end{bmatrix}\begin{bmatrix} \overline{\boldsymbol{V}^c} & \boldsymbol{0} \\ \boldsymbol{0} & \boldsymbol{V}^c \end{bmatrix} \tag{18}$$

where $\boldsymbol{V}^c = \mathrm{diag}\{V_i^c\} \in \mathbb{C}^{n\times n}$ and $V_i^c = V_i\angle\theta_i$ denotes the complex voltage of PQ bus i.

For better readability, the proof of Lemma 1 is given in the appendix. This lemma reveals the spectral equivalence between the power flow Jacobian and the new matrix $\widetilde{\boldsymbol{J}}$ for distribution systems with CP-DGs and CC-DGs. The matrix $\widetilde{\boldsymbol{J}}$ has an interesting structure that the admittance matrix of net loads and admittance matrix of the power network appear as sub-matrices. This property leads to the following theorem that reveals the relationship between the network-load admittance ratio and power

flow Jacobian singularity. Also, it will be shown later that the expression (18) leads to a convenient extension of the results to ZIP loads.

Theorem 1: The power flow Jacobian $\boldsymbol{J}_{pf}$ is singular if and only if the network-load admittance ratio $R_{n/d} = 1$.

Proof: Necessity. Suppose $\boldsymbol{J}_{pf}$ is singular. Since the matrix $\boldsymbol{V}^c$ in (18) is nonsingular, it follows from Lemma 1 that the matrix $\widetilde{\boldsymbol{Y}}$ is singular, where

$$\widetilde{\boldsymbol{Y}} = \begin{bmatrix} -\overline{\boldsymbol{Y}}_n & -\overline{\boldsymbol{Y}_d^{\text{eq}}} \\ \boldsymbol{Y}_d^{\text{eq}} & \boldsymbol{Y}_n \end{bmatrix} \in \mathbb{C}^{2n\times 2n}. \tag{19}$$

Then, there exist $\boldsymbol{a}, \boldsymbol{b} \in \mathbb{C}^n$, which are not both zero vectors, such that

$$\begin{aligned} -\overline{\boldsymbol{Y}}_n \boldsymbol{a} - \overline{\boldsymbol{Y}_d^{\text{eq}}} \boldsymbol{b} &= \boldsymbol{0} \\ \boldsymbol{Y}_d^{\text{eq}} \boldsymbol{a} + \boldsymbol{Y}_n \boldsymbol{b} &= \boldsymbol{0}. \end{aligned} \tag{20}$$

Since $(\overline{\boldsymbol{Y}_d^{\text{eq}}})^{-1} = \overline{(\boldsymbol{Y}_d^{\text{eq}})^{-1}}$, it follows from (20) that

$$\begin{aligned} (\overline{\boldsymbol{Y}_d^{\text{eq}}})^{-1}(-\overline{\boldsymbol{Y}}_n \boldsymbol{a} - \overline{\boldsymbol{Y}_d^{\text{eq}}} \boldsymbol{b}) &= \overline{\boldsymbol{Y}}_{n/d} \boldsymbol{a} + \boldsymbol{b} = \boldsymbol{0} \\ (\boldsymbol{Y}_d^{\text{eq}})^{-1}(\boldsymbol{Y}_d^{\text{eq}} \boldsymbol{a} + \boldsymbol{Y}_n \boldsymbol{b}) &= \boldsymbol{a} + \boldsymbol{Y}_{n/d} \boldsymbol{b} = \boldsymbol{0} \end{aligned} \tag{21}$$

and eliminating $\boldsymbol{b}$ in (21) gives

$$\boldsymbol{Y}_{n/d} \overline{\boldsymbol{Y}}_{n/d} \boldsymbol{a} = \boldsymbol{a}. \tag{22}$$

We claim that $\boldsymbol{a}$ and $\boldsymbol{b}$ are both nonzero, otherwise (21) leads to that $\boldsymbol{a}$, $\boldsymbol{b}$ are both zero vectors. Equation (22) implies that the matrix $\boldsymbol{Y}_{n/d}\overline{\boldsymbol{Y}}_{n/d}$ has an eigenvalue that is equal to one and the nonzero $\boldsymbol{a}$ is the corresponding eigenvector. So we have $R_{n/d} = 1$ by Definition 3.

Sufficiency. If $R_{n/d} = 1$, the matrix $\boldsymbol{Y}_{n/d}\overline{\boldsymbol{Y}}_{n/d}$ has an eigenvalue that is equal to one. Then, there exists a nonzero vector $\boldsymbol{a} \in \mathbb{C}^n$ such that $\boldsymbol{Y}_{n/d}\overline{\boldsymbol{Y}}_{n/d}\boldsymbol{a} = \boldsymbol{a}$. Let $\boldsymbol{b} = -\overline{\boldsymbol{Y}}_{n/d}\boldsymbol{a}$, it follows from $\overline{\boldsymbol{Y}}_{n/d} = (\overline{\boldsymbol{Y}_d^{\text{eq}}})^{-1}\overline{\boldsymbol{Y}}_n$ that

$$\begin{bmatrix} -\overline{\boldsymbol{Y}}_n & -\overline{\boldsymbol{Y}_d^{\text{eq}}} \\ \boldsymbol{Y}_d^{\text{eq}} & \boldsymbol{Y}_n \end{bmatrix} \begin{bmatrix} \boldsymbol{a} \\ \boldsymbol{b} \end{bmatrix} = \begin{bmatrix} -\overline{\boldsymbol{Y}}_n \boldsymbol{a} + \overline{\boldsymbol{Y}_d^{\text{eq}}} \overline{\boldsymbol{Y}}_{n/d} \boldsymbol{a} \\ \boldsymbol{Y}_d^{\text{eq}}(\boldsymbol{a} - \boldsymbol{Y}_{n/d}\overline{\boldsymbol{Y}}_{n/d}\boldsymbol{a}) \end{bmatrix} = \boldsymbol{0}. \tag{23}$$

It implies that $\widetilde{\boldsymbol{Y}}$ is singular so that $\boldsymbol{J}_{pf}$ is also singular by Lemma 1. ■

The singularity condition in Theorem 1 ($R_{n/d} = 1$) can be interpreted as a generalized admittance matching between the power network and net loads, i.e., the maximum loadability of the power network. For the single-load infinite-bus system, the condition $R_{n/d} = 1$ is reduced to $|Y_{d1}^{-1}Y_{12}| = 1$, which is equivalent to (14). So the theorem includes the criterion of the unity line-load admittance ratio as a special case. Also, we compare Theorem 1 with a recent relevant result. It is shown in [4] that $|V_i^c| \geq \sum_{j=1}^n |Z_{ij}I_j^c|$, $i = 1, ..., n$ is a sufficient condition for the power flow Jacobian non-singularity of distribution systems, where Z_{ij} denotes the (i, j) entry of the impedance matrix of the power network and I_j^c denotes the complex current injection at bus j. A variant of this inequality can be expressed by

$$|\widetilde{Y}_{Li}^{-1}\widetilde{Y}_{Ni}| \geq 1 \tag{24}$$

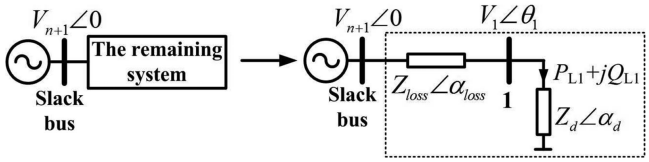

Fig. 3. A virtual two-bus system looking from the slack bus.

where $\widetilde{Y}_{Li} = \frac{I_i^c}{V_i^c}$ and $\widetilde{Y}_{Ni} = (\sum_{j=1}^n |\frac{I_j^c}{I_i^c}Z_{ij}|)^{-1}$. The left hand side of (24) is also a term in the manner of the network-load admittance ratio. By comparison, the proposed definition $R_{n/d}$ has a merit that it gives a necessary and sufficient condition for the power flow Jacobian singularity.

C. A New Voltage Stability Index

Inspired by Theorem 1, we propose a new voltage stability index in this subsection. For a given distribution system, let $R_{n/d}$ and

$$\begin{aligned} P_{loss} + \text{j}Q_{loss} &= \sum_{i=1}^{n+1} S_i \\ P_d + \text{j}Q_d &= -\sum_{i=1}^{n} S_i \end{aligned} \tag{25}$$

be the network-load admittance ratio, network loss and total net load, respectively. We can virtually regard the original distribution system as a two-bus system by looking from the slack bus (see Fig. 3 for illustration). In the virtual two-bus system, we set that the equivalent load impedance is $Z_d\angle\alpha_d$, line impedance is $Z_{loss}\angle\alpha_{loss}$ and $|Z_d| = R_{n/d}|Z_{loss}|$ where $\alpha_{loss} = \tan^{-1}\frac{Q_{loss}}{P_{loss}}$ and $\alpha_d = \tan^{-1}\frac{Q_d}{P_d}$. Thus, the two-bus system and the original distribution system have the same network loss power factor, net load power factor, and further, the same voltage stability limit point as their network-load admittance ratios coincide.

We analyze the two-bus system in detail. Direct calculation gives that

$$P_{L1} = \frac{V_{n+1}^2}{Z_{loss}} \frac{R_{n/d}\cos\alpha_d}{|1\angle\alpha_{loss} + R_{n/d}\angle\alpha_d|^2}. \tag{26}$$

Letting $R_{n/d} = 1$ in (26) gives the active power load at the voltage stability limit point

$$P_{L1}^{\lim} = \frac{V_{n+1}^2}{Z_{loss}} \frac{\cos\alpha_d}{|1\angle\alpha_{loss} + 1\angle\alpha_d|^2}. \tag{27}$$

Then, we establish the following voltage stability index in terms of $R_{n/d}$, α_{loss} and α_d

$$\begin{aligned} M_{n/d} &= 1 - \frac{P_{L1}}{P_{L1}^{\lim}} \\ &= 1 - \frac{R_{n/d}|1\angle\alpha_{loss} + 1\angle\alpha_d|^2}{|1\angle\alpha_{loss} + R_{n/d}\angle\alpha_d|^2}. \end{aligned} \tag{28}$$

Since $R_{n/d}$ approaches to infinity at the zero load case and $R_{n/d} = 1$ at the voltage stability limit point, the index $M_{n/d}$

ranges from 0 (stability limit point) to 1 (zero load case) and thus measures the voltage stability margin. We note that the index $M_{n/d}$ applies to the two-bus system as well as the original distribution system since they have the same voltage stability limit point as aforementioned.

From the above derivation, the index $M_{n/d}$ is perfectly linear with load increase if the original system is a single-load infinite-bus system (see that $M_{n/d}$ is linear with respect to P_{L1} in (28)). Further, it will be seen in case study that $M_{n/d}$ still preserves good linearity with load increase for generic distribution systems. It is desirable for stability monitoring, and a merit over the traditional indices that have nonlinear shapes (e.g., the minimum eigenvalue/singular value of power flow Jacobian). We refer to [34] for a more detailed discussion on the importance of stability index linearity.

IV. Extensions of the Obtained Results

The obtained results are based on a balanced three-phase distribution system with constant-power loads, CP-DGs and CC-DGs. They can be further extended to more general and practical cases with some minor modifications. We discuss some of the possible extensions below.

1) ZIP Loads. Suppose the loads in (1) are in ZIP form, i.e.,

$$\begin{aligned} P_{Li}(V_i) &= a_{pi}V_i^2 + b_{pi}V_i + c_{pi} \\ Q_{Li}(V_i) &= a_{qi}V_i^2 + b_{qi}V_i + c_{qi} \end{aligned} \tag{29}$$

where a_{pi}, b_{pi}, c_{pi} (a_{qi}, b_{qi}, c_{qi}) are the coefficients for active (reactive) power load at bus i. The quadratic terms $a_{pi}V_i^2, a_{qi}V_i^2$ refer to the "Z" component, which can be regarded as an additional shunt admittance at bus i. The linear terms $b_{pi}V_i$, $b_{qi}V_i$ refer to the "I" component, which can be regarded as a CC-DG with negative current injection. Thus, the power flow equations with ZIP loads can be reformulated as

$$\begin{aligned} 0 = {} & V_i^2\widetilde{G}_{ii} + \sum_{j\in\mathcal{N}_i} V_iV_j|Y_{ij}|\sin(\theta_{ij}-\varphi_{ij}) \\ & - P_{Gi}^{\mathrm{CP}} - \widetilde{I}_{pi}^{\mathrm{CC}}V_i + c_{pi} \\ 0 = {} & -V_i^2\widetilde{B}_{ii} - \sum_{j\in\mathcal{N}_i} V_iV_j|Y_{ij}|\cos(\theta_{ij}-\varphi_{ij}) \\ & - Q_{Gi}^{\mathrm{CP}} - \widetilde{I}_{qi}^{\mathrm{CC}}V_i + c_{qi} \end{aligned} \tag{30}$$

where $\widetilde{G}_{ii} = G_{ii} + a_{pi}$, $\widetilde{B}_{ii} = B_{ii} + a_{qi}$, $\widetilde{I}_{pi}^{\mathrm{CC}} = I_{pi}^{\mathrm{CC}} - b_{pi}$ and $\widetilde{I}_{qi}^{\mathrm{CC}} = I_{qi}^{\mathrm{CC}} - b_{qi}$. Observing (1), (18) and (30), the obtained results still apply by replacing $G_{ii}, B_{ii}, I_{pi}^{\mathrm{CC}}, I_{qi}^{\mathrm{CC}}$ with $\widetilde{G}_{ii}, \widetilde{B}_{ii}, \widetilde{I}_{pi}^{\mathrm{CC}}, \widetilde{I}_{qi}^{\mathrm{CC}}$ in the definitions of $\boldsymbol{Y}_n$ and $\boldsymbol{Y}_d^{\mathrm{eq}}$.

2) Unbalanced Three-Phase Distribution Systems. For a generic three-phase distribution system, the power flow equations for each single phase of a PQ bus can also be formulated as (1) by interpreting $\theta_i, V_i, P_i, Q_i, Y_{ij}$ as single phase variables. Then, we have $3n$ equations to describe active and reactive power flows for PQ buses, respectively. Given the three-phase complex voltages of the slack bus, we still obtain the power flow Jacobian as the form of (3) where $\boldsymbol{J}_{P\theta}, \boldsymbol{J}_{PV}, \boldsymbol{J}_{Q\theta}, \boldsymbol{J}_{QV}$ are $3n$ by $3n$ matrices. Thus the obtained results still apply.

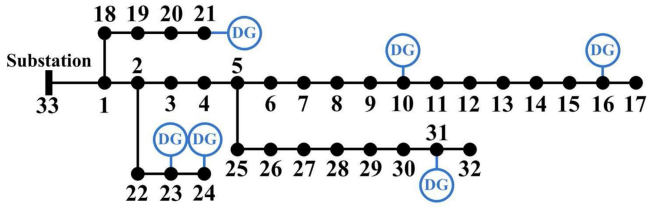

Fig. 4. Diagram of the modified IEEE 33-bus system.

3) Mesh Power Networks. The proofs of Lemma 1 and Theorem 1 take no assumptions on the power network topology and R/X ratio of transmission lines. Therefore, the obtained results apply to not only radial distribution systems but also mesh power systems without PV buses, such as microgrids and sub-transmission systems with renewable energy. Also, the results have potential applications in transmission systems in a possible future scenario such that all the sources are inverter-interfaced [35]. In the case study, we will have a test on a modified IEEE 30-bus system, which has mesh topology, as an illustration.

Moreover, we note that Lemma 1 and Theorem 1 are generally not true for power systems where PV buses do exist. The presence of PV buses makes the matrices $\boldsymbol{J}_{Q\theta}$ and $\boldsymbol{J}_{PV}$ no longer square, so that the previous analysis does not hold. Nevertheless, we will give a numerical example on IEEE 118-bus system (with 53 PV buses) in the case study. It shows that the proposed index $M_{n/d}$ still provides useful information on stability evaluation for this system. On the other hand, a rigorous extension to power systems with PV buses is beyond the scope of this paper and will be considered in future work.

V. Case Study

A. Verification of the Proposed Index

We take a modified IEEE 33-bus system to verify the obtained results. The system diagram is depicted in Fig. 4, and we refer to [36] for load and network parameters. Assume the loads are constant-power loads, and six DGs are connected to bus 10, 16, 21, 23, 24 and 31, respectively. Each DG has $k \cdot 0.6192$ MVA capacity and operates at unity power factor. We refer to the scala k as the DG penetration level. Note that the total active load in the base case is 3.715 MW, so the case of $k = 1$ implies that the active load is 100% carried by the six DGs. We set the following four scenarios with different load increase directions, DG penetration levels and control modes:

1) 0% DG penetration, loads increase proportionally to their base values;
2) 0% DG penetration, a randomly selected load increase direction;
3) 50% CP-DG penetration, loads increase proportionally to their base values;
4) 50% CC-DG penetration, loads increase proportionally to their base values.

In each scenario, we trace power flow solutions till the singularity point by using the CPF [7]. The curves of $R_{n/d}$ are shown in Fig. 5, where the coefficient μ is the ratio of the total load increment to total base load that represents load level. We have

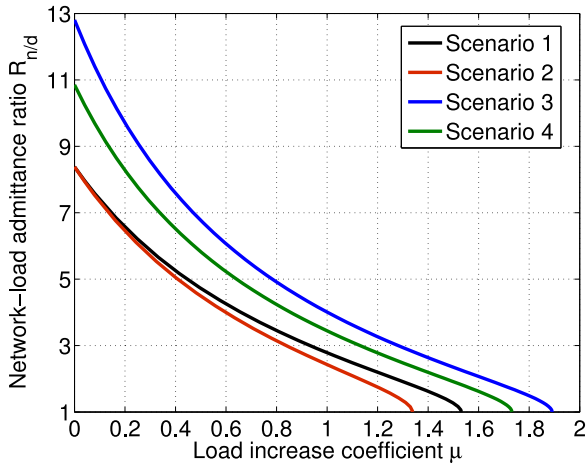

Fig. 5. The modified IEEE 33-bus system: $R_{n/d}$ with load increase.

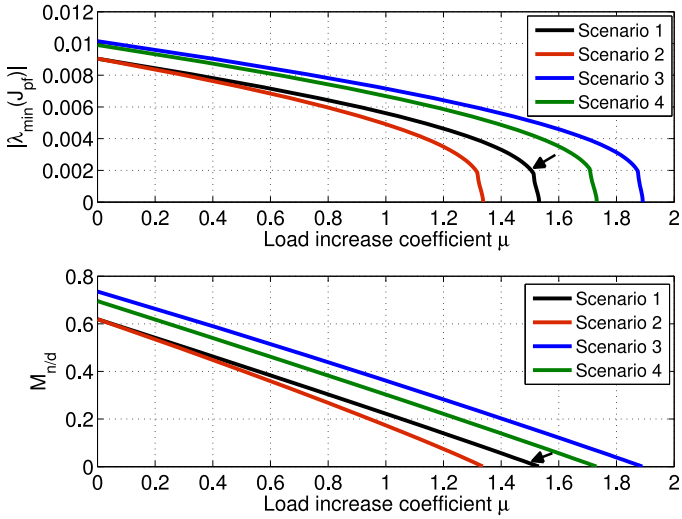

Fig. 6. The modified IEEE 33-bus system: The indices with load increase.

$R_{n/d} = 1$ at the voltage stability limit point in each scenario, which coincides with Theorem 1.

We compare the performance of the new index $M_{n/d}$ with a traditional index $|\lambda_{\min}(\boldsymbol{J}_{pf})|$ [2]. The curves of the two indices in these four scenarios are depicted in Fig. 6. At the voltage stability limit point in each scenario, $|\lambda_{\min}(\boldsymbol{J}_{pf})|$ is exactly zero by its definition, and $M_{n/d}$ also decreases to zero as expected. In addition, we observe that the curve of $|\lambda_{\min}(\boldsymbol{J}_{pf})|$ deviates from linearity in a concave manner. It keeps a flat slope for a wide interval and sharply decrease to zero just before the voltage stability limit, which is an undesirable property. Consider the point on the curve in scenario 1 at $\mu = 1.5$ (see the black arrow in Fig. 6). At this point, the system is very close to the stability limit. However, the corresponding $|\lambda_{\min}(\boldsymbol{J}_{pf})|$ is around 20% of its value in the base case, which may give a false information that the system still has some stability margin. By comparison, the curve of $M_{n/d}$ is highly linear with load increase and thus performs much better on stability monitoring and stability margin estimation. Also, according to the discussion on computing $R_{n/d}$ in Section III, the index $M_{n/d}$ can be efficiently solved

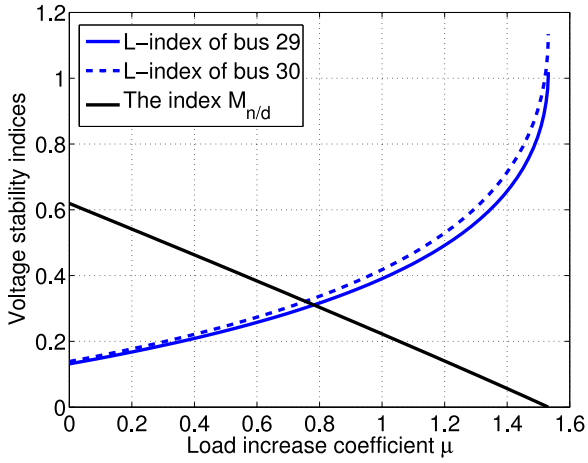

Fig. 7. The modified IEEE 33-bus system: Comparison of $M_{n/d}$ and L-index in Scenario 1.

and hence adequate for online application. The computational cost of $M_{n/d}$ is lower than that of $|\lambda_{\min}(\boldsymbol{J}_{pf})|$ as the concerned matrix $\boldsymbol{Y}_{n/d}\overline{\boldsymbol{Y}}_{n/d}$ has half the dimension of $\boldsymbol{J}_{pf}$.

Next, we compare $M_{n/d}$ with the L-index, which is another commonly used index. Different from the system-wide index $|\lambda_{\min}(\boldsymbol{J}_{pf})|$, the L-index is in local type, i.e., it is defined on each bus. The L-indices of bus 29 and bus 30 in Scenario 1 are plotted in Fig. 7. These two buses are weak points in the system as they are close to feeder ends and connect big loads. The corresponding indices are greater than one around $\mu = 1.5$, which indicates the proximity to voltage stability limit. However, the L-index has parabolic shape and the stability criterion of L-index being less than one is rigorous only in special case [4]. It again highlights the merits of $M_{n/d}$ that has good linearity and holds true for general cases.

We set up the following experiment to further check the linearity of $M_{n/d}$. We select two points on the curve of $M_{n/d}$. Let $(0, M^0_{n/d})$ denote the point at the base load level, and $(\mu_1, M^1_{n/d})$ denote the point at the load level μ_1. Then, the load increase coefficient at the stability limit point can be linearly estimated by $\mu^{\lim}_{est} = \frac{\mu_1 M^0_{n/d}}{M^0_{n/d} - M^1_{n/d}}$. We gradually increase μ_1 from zero to its maximum, and take the point $(\mu_1, M^1_{n/d})$ for the estimation. The error statistics in Fig. 8 shows that this simple estimator already achieves a satisfactory performance, which verifies the good linearity of $M_{n/d}$. The error is within 10% when the system status is still far away from the stability limit. It implies that the index $M_{n/d}$ is able to provide a good estimation even at an early stage.

Moreover, we test the indices on a modified IEEE 123-bus system (radial feeder) and a modified IEEE 30-bus system (mesh network). The system diagrams are omitted here, and we refer to the file "case_ieee123_ug.m" [37] and "case_ieee30.m" [38] for the detailed parameters. We regard all generator buses but the slack bus in the modified IEEE 30-bus system as PQ buses with constant-power injection 15+j10 MVA. Fig. 9 and Fig. 10 show the curves of the two indices in the following two scenarios:

1) Loads increase proportionally to their base values;
2) A randomly selected load increase direction.

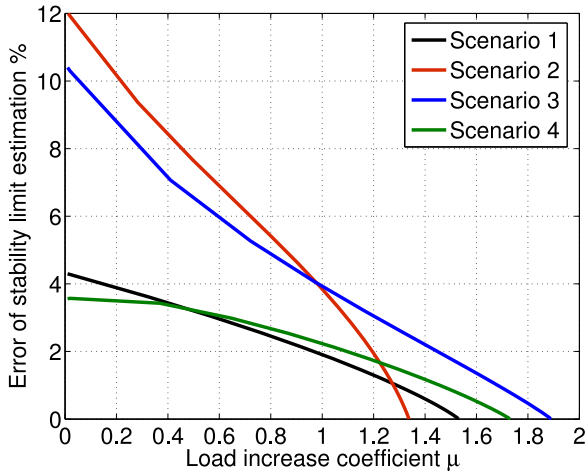

Fig. 8. The modified IEEE 33-bus system: Error of stability limit estimation.

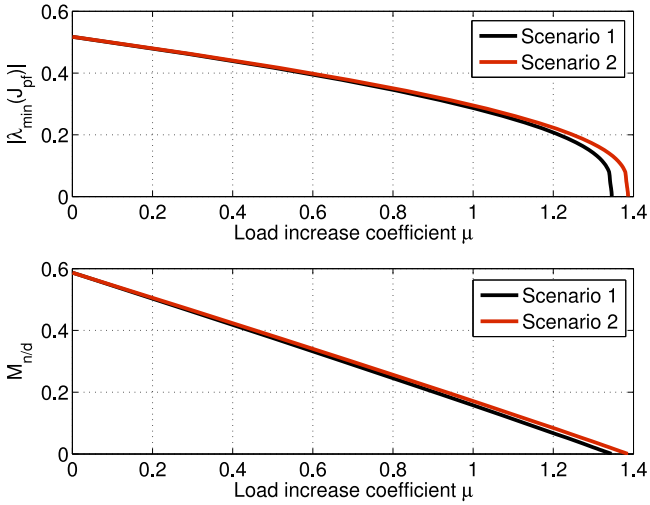

Fig. 9. The modified IEEE 123-bus system: The indices with load increase.

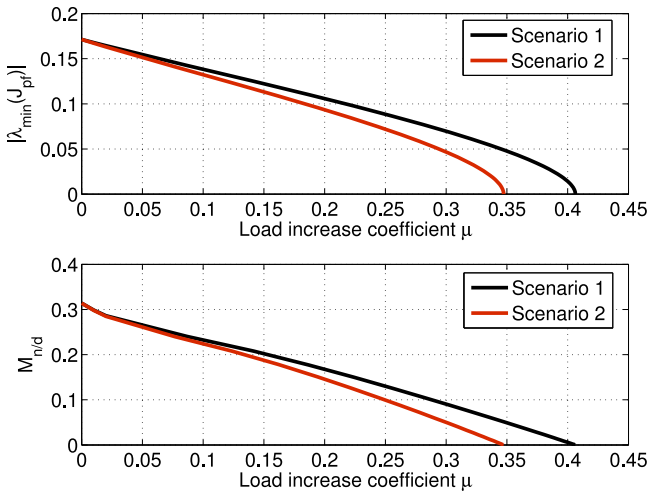

Fig. 10. The modified IEEE 30-bus system: The indices with load increase.

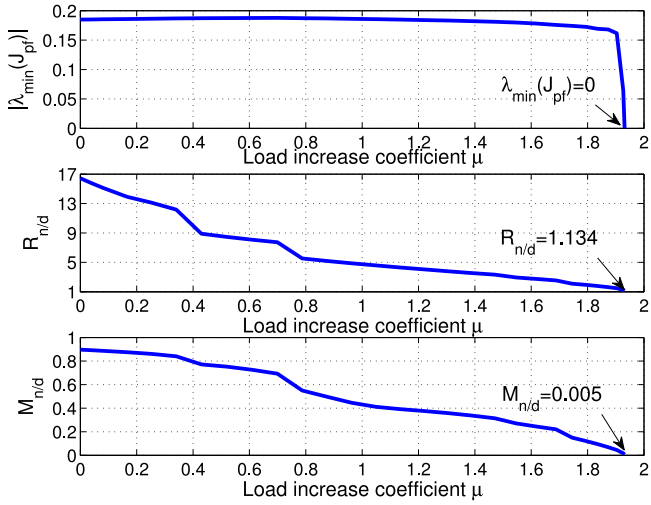

Fig. 11. IEEE 118-bus system: The indices with load increase.

Note that these two systems have some tie buses and we set $Y_{di}^{\text{eq}} = \epsilon$ for those tie buses. It turns out that the index $M_{n/d}$ still works well with the perturbation, and the curve shape is similar to the case of IEEE 33-bus system. For the 123-bus system, the curve of $M_{n/d}$ has good linearity in the whole interval. For the 30-bus system, the curve of $M_{n/d}$ slightly deviates from linearity in a convex manner in the interval $0 \leq \mu \leq 0.1$. In the remaining interval, which corresponds to heavy load cases and is of more interest for stability monitoring, the index is close to linearity and has a good performance.

Furthermore, we test the proposed index on the IEEE 118-bus system that has 53 generators as PV buses (referring to "case118.m" [38] for the system parameters). The curves of $|\lambda_{\min}(\boldsymbol{J}_{pf})|$, $R_{n/d}$ and $M_{n/d}$ are shown in Fig. 11, where we set that the loads increase proportionally to their base values and generators balance the load increment proportionally to their active power reserves. Note that the dimension of power flow Jacobian changes with the load level since some PV buses are switched to PQ buses when the corresponding generators hit their reactive power limits. It impacts the linearity of $M_{n/d}$ and causes a ladder-like shape. As aforementioned, the existence of PV buses makes $R_{n/d} = 1$ and $M_{n/d} = 0$ no longer hold at the voltage stability limit point. Nevertheless, we still observe that $M_{n/d}$ monotonically decreases with μ and gives quite precise evaluation around the stability limit. This is due to that the influence of PV buses is significantly reduced in heavy load case as many PV buses are switched to PQ buses. A systematic analysis of this issue remains to be done in the future.

B. The Impact of DG Penetration and Control Mode

In this subsection, we use the new index $M_{n/d}$ to study how the penetration level and control mode of DGs affect voltage stability. Assume the six DGs in the IEEE 33-bus system have the same parameters as in the previous subsection. The following two scenarios are set for comparison:

1) All DGs operate in CP mode. We obtain 101 power flow solutions by increasing the penetration level k from 0% to 100%

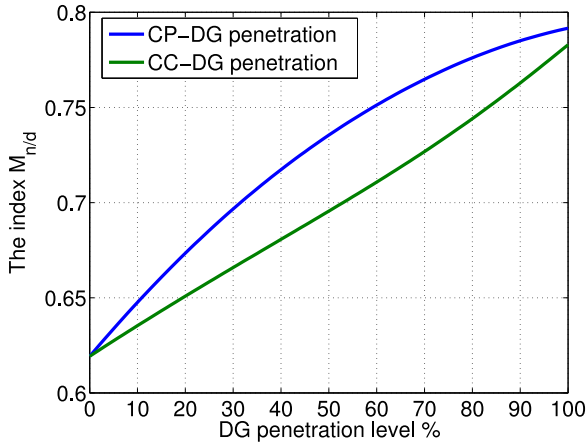

Fig. 12. $M_{n/d}$ with different DG penetration levels and control modes.

with a step size 1%. The corresponding voltage stability indices are calculated, denoted as $M_{n/d}^{\mathrm{CP}}$.

2) For the power flow solution at each penetration level k in the first scenario, we keep the solution $(\boldsymbol{\theta}, \boldsymbol{V})$ unchanged but switch all DGs to CC mode. This can be achieved by setting the current constants of the DG at bus i as $I_{pi}^{\mathrm{CC}} = \frac{k \cdot 0.6192}{V_i}$, $I_{qi}^{\mathrm{CC}} = 0$. Then the corresponding voltage stability indices are calculated, denoted as $M_{n/d}^{\mathrm{CC}}$.

Since the DG outputs can be regarded as negative loads, the voltage stability level is expected to grow with DG penetration level. The curves of $M_{n/d}^{\mathrm{CP}}$ and $M_{n/d}^{\mathrm{CC}}$ in Fig. 12 coincide with this expectation. Also, it should be pointed out that over-voltage phenomena are observed at some buses when the penetration level exceeds 75%. So the allowable DG penetration level in practice may not be as high as 100% in order to satisfy operation constraints. Furthermore, CP-DGs have better performance than CC-DGs in the entire interval in Fig. 12. It coincides with the fact that the system with CC-DGs has less loadability since the voltage drop in heavy load case will reduce the power injections of CC-DGs and deteriorate voltage stability.

VI. Conclusion

The well known voltage stability criterion of the unity line-load admittance ratio in the single-load infinite-bus system has been extended to generic distribution systems. We have defined the concept of the network-load admittance ratio. This concept is a generalization of the line-load admittance ratio that characterizes the loading status of a generic distribution system with the effects of CP-DGs and CC-DGs being considered. We have proved that the power flow Jacobian is singular if and only if the network-load admittance ratio is unity. This necessary and sufficient condition includes the criterion of the unity line-load admittance ratio as a special case. Based on this result, we have proposed a new voltage stability index, which is shown to be highly linear with load increase under various test scenarios. The proposed index can give good estimation of voltage stability margin and reflect the impact of DG penetration level and control mode on voltage stability.

Appendix
Proof of Lemma 1

Proof: First, according to (1), (2) and (4)–(7), the entries of $\boldsymbol{J}_{P\theta}, \boldsymbol{J}_{PV}, \boldsymbol{J}_{Q\theta}, \boldsymbol{J}_{QV}$ can be rewritten as follows

$$(\boldsymbol{J}_{P\theta})_{ij} = \begin{cases} -Q_i - V_i^2 B_{ii}, \, i = j \\ -V_i V_j |Y_{ij}| \cos(\theta_{ij} - \varphi_{ij}), \, i \neq j \end{cases} \tag{31}$$

$$(\boldsymbol{J}_{PV})_{ij} = \begin{cases} P_i + V_i^2 G_{ii} - I_{pi}^{\mathrm{CC}} V_i, \, i = j \\ V_i V_j |Y_{ij}| \sin(\theta_{ij} - \varphi_{ij}), \, i \neq j \end{cases} \tag{32}$$

$$(\boldsymbol{J}_{Q\theta})_{ij} = \begin{cases} P_i - V_i^2 G_{ii}, \, i = j \\ -V_i V_j |Y_{ij}| \sin(\theta_{ij} - \varphi_{ij}), \, i \neq j \end{cases} \tag{33}$$

$$(\boldsymbol{J}_{QV})_{ij} = \begin{cases} Q_i - V_i^2 B_{ii} - I_{qi}^{\mathrm{CC}} V_i, \, i = j \\ -V_i V_j |Y_{ij}| \cos(\theta_{ij} - \varphi_{ij}), \, i \neq j. \end{cases} \tag{34}$$

Assume the rows and columns of $\boldsymbol{J}_{pf}$ are indexed by $\mathcal{I}_0 = \{1, 2, ..., n, 1', 2', ..., n'\}$. Then, we rearrange the rows and columns of $\boldsymbol{J}_{pf}$ into a new index order $\mathcal{I}_1 = \{1, 1', 2, 2', ..., n, n'\}$, and denote the rearranged matrix as $\boldsymbol{J}_1$. By (31)–(34), the rearranged matrix $\boldsymbol{J}_1$ has the following form

$$\boldsymbol{J}_1 = \begin{bmatrix} \boldsymbol{A}_{11} & \boldsymbol{A}_{12} & \cdots & \boldsymbol{A}_{1n} \\ \boldsymbol{A}_{21} & \boldsymbol{A}_{22} & \cdots & \boldsymbol{A}_{2n} \\ \vdots & \vdots & \ddots & \vdots \\ \boldsymbol{A}_{n1} & \boldsymbol{A}_{n2} & \cdots & \boldsymbol{A}_{nn} \end{bmatrix} \tag{35}$$

where $\boldsymbol{A}_{ii}, i = 1, 2, ..., n$ takes value as

$$\begin{aligned} \boldsymbol{A}_{ii} &= \begin{bmatrix} (\boldsymbol{J}_{pf})_{ii} & (\boldsymbol{J}_{pf})_{ii'} \\ (\boldsymbol{J}_{pf})_{i'i} & (\boldsymbol{J}_{pf})_{i'i'} \end{bmatrix} = \begin{bmatrix} (\boldsymbol{J}_{P\theta})_{ii} & (\boldsymbol{J}_{PV})_{ii} \\ (\boldsymbol{J}_{Q\theta})_{ii} & (\boldsymbol{J}_{QV})_{ii} \end{bmatrix} \\ &= \begin{bmatrix} -Q_i - V_i^2 B_{ii} & P_i + V_i^2 G_{ii} - I_{pi}^{\mathrm{CC}} V_i \\ P_i - V_i^2 G_{ii} & Q_i - V_i^2 B_{ii} - I_{qi}^{\mathrm{CC}} V_i \end{bmatrix} \end{aligned} \tag{36}$$

and $\boldsymbol{A}_{ij}, i, j = 1, 2, ..., n, i \neq j$, takes value as

$$\begin{aligned} \boldsymbol{A}_{ij} &= \begin{bmatrix} (\boldsymbol{J}_{pf})_{ij} & (\boldsymbol{J}_{pf})_{ij'} \\ (\boldsymbol{J}_{pf})_{i'j} & (\boldsymbol{J}_{pf})_{i'j'} \end{bmatrix} = \begin{bmatrix} (\boldsymbol{J}_{P\theta})_{ij} & (\boldsymbol{J}_{PV})_{ij} \\ (\boldsymbol{J}_{Q\theta})_{ij} & (\boldsymbol{J}_{QV})_{ij} \end{bmatrix} \\ &= V_i V_j |Y_{ij}| \begin{bmatrix} -\cos(\theta_{ij} - \varphi_{ij}) & \sin(\theta_{ij} - \varphi_{ij}) \\ -\sin(\theta_{ij} - \varphi_{ij}) & -\cos(\theta_{ij} - \varphi_{ij}) \end{bmatrix}. \end{aligned} \tag{37}$$

The above operation is equivalent to the elementary transform

$$\boldsymbol{J}_1 = \boldsymbol{E}_r \boldsymbol{J}_{pf} \boldsymbol{E}_r^{-1} \tag{38}$$

where $\boldsymbol{E}_r \in \mathbb{R}^{2n \times 2n}$ is the row switching matrix that changes the row order of $\boldsymbol{J}_{pf}$ from $\mathcal{I}_0$ to $\mathcal{I}_1$.

Then, it can be checked that the following decompositions hold for $\boldsymbol{A}_{ii}, i = 1, 2, ..., n$ and $\boldsymbol{A}_{ij}, i, j = 1, 2, ..., n, i \neq j$

$$\boldsymbol{A}_{ii} = \boldsymbol{U} \boldsymbol{D}_{ii} \boldsymbol{U}^{-1}, \; \boldsymbol{A}_{ij} = \boldsymbol{U} \boldsymbol{D}_{ij} \boldsymbol{U}^{-1} \tag{39}$$

where $\boldsymbol{U} = \frac{\sqrt{2}}{2}\begin{bmatrix} 1 & 1 \\ -\mathrm{j} & \mathrm{j} \end{bmatrix}$, $\boldsymbol{U}^{-1} = \frac{\sqrt{2}}{2}\begin{bmatrix} 1 & \mathrm{j} \\ 1 & -\mathrm{j} \end{bmatrix}$ and

$$\boldsymbol{D}_{ii} = \mathrm{j}\begin{bmatrix} -V_i^c(\overline{\boldsymbol{Y}}_n)_{ii}\overline{V_i^c} & -V_i^c(\overline{\boldsymbol{Y}_d^{\mathrm{eq}}})_{ii}V_i^c \\ \overline{V_i^c}(\boldsymbol{Y}_d^{\mathrm{eq}})_{ii}\overline{V_i^c} & \overline{V_i^c}(\boldsymbol{Y}_n)_{ii}V_i^c \end{bmatrix}$$

$$\boldsymbol{D}_{ij} = \mathrm{j}\begin{bmatrix} -V_i^c(\overline{\boldsymbol{Y}}_n)_{ij}\overline{V_j^c} & 0 \\ 0 & \overline{V_i^c}(\boldsymbol{Y}_n)_{ij}V_j^c \end{bmatrix}. \quad (40)$$

By (35) and (39), the matrix $\boldsymbol{J}_1$ can be re-expressed as

$$\boldsymbol{J}_1 = (\boldsymbol{I}_n \otimes \boldsymbol{U})\boldsymbol{D}(\boldsymbol{I}_n \otimes \boldsymbol{U})^{-1} \quad (41)$$

where $\otimes$ denotes Kronecker product and

$$\boldsymbol{D} = \begin{bmatrix} \boldsymbol{D}_{11} & \cdots & \boldsymbol{D}_{1n} \\ \vdots & \ddots & \vdots \\ \boldsymbol{D}_{n1} & \cdots & \boldsymbol{D}_{nn} \end{bmatrix}. \quad (42)$$

Further, assume the rows and columns of $\boldsymbol{D}$ are indexed by $\mathcal{I}_1 = \{1, 1', 2, 2', ..., n, n'\}$. We rearrange them into a new order $\mathcal{I}_0 = \{1, 2, ..., n, 1', 2', ..., n'\}$, which is equivalent to the elementary transform $\boldsymbol{E}_r^{-1}\boldsymbol{D}\boldsymbol{E}_r$. Observing (18), (40) and (42) gives

$$\widetilde{\boldsymbol{J}} = \boldsymbol{E}_r^{-1}\boldsymbol{D}\boldsymbol{E}_r. \quad (43)$$

Thus, from (38), (41) and (43) we conclude that

$$\boldsymbol{J}_{pf} = \boldsymbol{E}_r^{-1}(\boldsymbol{I}_n \otimes \boldsymbol{U})\boldsymbol{E}_r\widetilde{\boldsymbol{J}}\boldsymbol{E}_r^{-1}(\boldsymbol{I}_n \otimes \boldsymbol{U})^{-1}\boldsymbol{E}_r \quad (44)$$

which implies that $\widetilde{\boldsymbol{J}}$ is similar to $\boldsymbol{J}_{pf}$.

REFERENCES

[1] T. Van Cutsem and C. Vournas, *Voltage Stability of Electric Power Systems*. New York, NY, USA: Springer, 1998.

[2] C. A. Canizares, "Voltage stability assessment: Concepts, practices and tools," *IEEE/PES Power System Stability Subcommittee, Piscataway, NJ, USA, Tech. Rep. PES-TR9*, Aug. 2002.

[3] S. Bolognani and S. Zampieri, "On the existence and linear approximation of the power flow solution in power distribution networks," *IEEE Trans. Power Syst.*, vol. 31, no. 1, pp. 163–172, Jan. 2016.

[4] Z. Wang, B. Cui, and J. Wang, "A necessary condition for power flow insolvability in power distribution systems with distributed generators," *IEEE Trans. Power Syst.*, vol. 32, no. 2, pp. 1440–1450, Mar. 2017.

[5] L. Aolaritei, S. Bolognani, and F. Dörfler, "Hierarchical and distributed monitoring of voltage stability in distribution networks," *IEEE Trans. Power Syst.*, vol. 33, no. 6, pp. 6705–6714, Nov. 2018.

[6] S. Iwamoto and Y. Tamura, "A load flow calculation method for ill-conditioned power systems," *IEEE Trans. Power App. Syst.*, vol. PAS-100, no. 4, pp. 1736–1743, Apr. 1981.

[7] V. Ajjarapu and C. Christy, "The continuation power flow: A tool for steady state voltage stability analysis," *IEEE Trans. Power Syst.*, vol. 7, no. 1, pp. 416–423, Feb. 1992.

[8] H. Sheng and H.-D. Chiang, "CDFLOW: A practical tool for tracing stationary behaviors of general distribution networks," *IEEE Trans. Power Syst.*, vol. 29, no. 3, pp. 1365–1371, May 2014.

[9] A. Trias, "The holomorphic embedding load flow method," in *Proc. IEEE Power Energy Soc. Gen. Meeting*, Jul. 2012, pp. 1–8.

[10] F. Echavarren, E. Lobato, L. Rouco, and T. Gmez, "Formulation, computation and improvement of steady state security margins in power systems. Part I: Theoretical framework," *Int. J. Elect. Power Energy Syst.*, vol. 33, no. 2, pp. 340–346, 2011.

[11] F. Echavarren, E. Lobato, L. Rouco, and T. Gmez, "Formulation, computation and improvement of steady state security margins in power systems. Part II: Results," *Int. J. Elect. Power Energy Syst.*, vol. 33, no. 2, pp. 347–358, 2011.

[12] B. Gao, G. Morison, and P. Kundur, "Voltage stability evaluation using modal analysis," *IEEE Trans. Power Syst.*, vol. 7, no. 4, pp. 1529–1542, Nov. 1992.

[13] P. A. Löf, G. Andersson, and D. J. Hill, "Voltage stability indices for stressed power systems," *IEEE Trans. Power Syst.*, vol. 8, no. 1, pp. 326–335, Feb. 1993.

[14] I. Dobson, "Observations on the geometry of saddle node bifurcation and voltage collapse in electrical power systems," *IEEE Trans. Circuits Syst. I*, vol. 39, no. 3, pp. 240–243, Mar. 1992.

[15] A. Calvaer, "On the maximum loading of active linear electric multiports," *Proc. IEEE*, vol. WC-71, no. 2, pp. 282–283, Feb. 1983.

[16] K. Vu, M. M. Begovic, D. Novosel, and M. M. Saha, "Use of local measurements to estimate voltage-stability margin," *IEEE Trans. Power Syst.*, vol. 14, no. 3, pp. 1029–1035, Aug. 1999.

[17] B. Milosevic and M. Begovic, "Voltage-stability protection and control using a wide-area network of phasor measurements," *IEEE Trans. Power Syst.*, vol. 18, no. 1, pp. 121–127, Feb. 2003.

[18] I. Smon, G. Verbic, and F. Gubina, "Local voltage-stability index using Tellegen's theorem," *IEEE Trans. Power Syst.*, vol. 21, no. 3, pp. 1267–1275, Aug. 2006.

[19] S. Corsi and G. N. Taranto, "A real-time voltage instability identification algorithm based on local phasor measurements," *IEEE Trans. Power Syst.*, vol. 23, no. 3, pp. 1271–1279, Aug. 2008.

[20] Y. Wang *et al.*, "Voltage stability monitoring based on the concept of coupled single-port circuit," *IEEE Trans. Power Syst.*, vol. 26, no. 4, pp. 2154–2163, Nov. 2011.

[21] G. Jasmon and L. Lee, "Distribution network reduction for voltage stability analysis and loadflow calculations," *Int. J. Elect. Power Energy Syst.*, vol. 13, no. 1, pp. 9–13, 1991.

[22] M. Chakravorty and D. Das, "Voltage stability analysis of radial distribution networks," *Int. J. Elect. Power Energy Syst.*, vol. 23, no. 2, pp. 129–135, 2001.

[23] J. Yu, W. Li, V. Ajjarapu, W. Yan, and X. Zhao, "Identification and location of long-term voltage instability based on branch equivalent," *IET Gener. Transmiss. Distrib.*, vol. 8, no. 1, pp. 46–54, Jan. 2014.

[24] P. Kessel and H. Glavitsch, "Estimating the voltage stability of a power system," *IEEE Trans. Power Del.*, vol. PWRD-1, no. 3, pp. 346–354, Jul. 1986.

[25] M. Ilic, "Network theoretic conditions for existence and uniqueness of steady state solutions to electric power circuits," in *Proc. IEEE Int. Symp. Circuits Syst.*, 1992, vol. 6, pp. 2821–2828.

[26] J. W. Simpson-Porco, F. Dörfler, and F. Bullo, "Voltage collapse in complex power grids," *Nature Commun.*, vol. 7, 2016, Art. no. 10790.

[27] S. Grijalva, "Individual branch and path necessary conditions for saddle-node bifurcation voltage collapse," *IEEE Trans. Power Syst.*, vol. 27, no. 1, pp. 12–19, Feb. 2012.

[28] H.-D. Chiang and M. E. Baran, "On the existence and uniqueness of load flow solution for radial distribution power networks," *IEEE Trans. Circuits Syst.*, vol. 37, no. 3, pp. 410–416, Mar. 1990.

[29] K. N. Miu and H.-D. Chiang, "Existence, uniqueness, and monotonic properties of the feasible power flow solution for radial three-phase distribution networks," *IEEE Trans. Circuits Syst. I*, vol. 47, no. 10, pp. 1502–1514, Oct. 2000.

[30] C. Wang, A. Bernstein, J.-Y. Le Boudec, M. Paolone, "Explicit conditions on existence and uniqueness of load-flow solutions in distribution networks," *IEEE Trans. Smart Grid*, vol. 9, no. 2, pp. 953–962, Mar. 2018.

[31] Z. Ye, R. Walling, L. Garces, R. Zhou, L. Li, and T. Wang, "Study and development of anti-islanding control for grid-connected inverters," , Nat. Renew. Energy Lab., Golden, CO, USA, Tech. Rep. NREL/SR-560-36243, 2004.

[32] F. Dörfler and F. Bullo, "Kron reduction of graphs with applications to electrical networks," *IEEE Trans. Circuits Syst. I*, vol. 60, no. 1, pp. 150–163, Jan. 2013.

[33] Y. Saad, *Numerical Methods for Large Eigenvalue Problems: Revised Edition*. Philadelphia, PA, USA: SIAM, 2011.

[34] A. R. R. Matavalam and V. Ajjarapu, "Calculating the long term voltage stability margin using a linear index," in *Proc. IEEE Power Energy Soc. Gen. Meeting*, 2015, pp. 1–5.

[35] D. Ramasubramanian, V. Vittal, and J. M. Undrill, "Transient stability analysis of an all converter interfaced generation WECC system," in *Proc. Power Syst. Comput. Conf.*, 2016, pp. 1–7.

[36] M. E. Baran and F. F. Wu, "Network reconfiguration in distribution systems for loss reduction and load balancing," *IEEE Trans. Power Del.*, vol. 4, no. 2, pp. 1401–1407, Apr. 1989.

[37] S. Bolognani, "Approximate linear solution of power flow equations in power distribution networks, GitHub," 2014. [Online]. Available: http://github.com/saveriob/approx-pf
[38] R. D. Zimmerman, C. E. Murillo-Sánchez, and R. J. Thomas, "MATPOWER: Steady-state operations, planning, and analysis tools for power systems research and education," *IEEE Trans. Power Syst.*, vol. 26, no. 1, pp. 12–19, Feb. 2011.

Yue Song (M'14) received the B.S. and M.S. degrees from Shanghai Jiao Tong University, Shanghai, China, in 2011 and 2014, respectively, and the Ph.D. degree from The University of Hong Kong, Hong Kong, in 2017, all in electrical engineering. He is currently a Postdoctoral Fellow with the Department of Electrical and Electronic Engineering, The University of Hong Kong. His research interests include power systems, stability analysis, and dynamical networks. During his Ph.D. studies, he received the Hong Kong Ph.D. Fellowship from the Research Grants Council of Hong Kong and CLP Fellowship in electrical engineering from The University of Hong Kong.

David J. Hill (M'76–SM'91–F'93–LF'14) received the B.E. degree in electrical engineering and the B.Sc. degree in mathematics degrees from The University of Queensland, Brisbane, QLD, Australia, in 1972 and 1974, respectively, and the Ph.D. degree in electrical engineering from The University of Newcastle, Callaghan, NSW, Australia, in 1976.

During 1996–1999 and 2001–2004, he was the Head of the respective departments in Sydney and Hong Kong. Since 1994, he been has holding various positions with The University of Sydney, Sydney, NSW, Australia, including the Chair of Electrical Engineering until 2002 and again during 2010–2013, along with an ARC Professorial Fellowship. He is currently the Chair of electrical engineering with the Department of Electrical and Electronic Engineering, The University of Hong Kong, Hong Kong. He currently holds honorary professorships with the City University of Hong Kong, Hong Kong, with the South China University of Technology, Guangzhou, China, with Wuhan University, Wuhan, China, and with Northeastern University, Shenyang, China. He is also a part-time Professor with the Centre for Future Energy Networks, The University of Sydney. He has also held academic and substantial visiting positions with The University of Melbourne, Parkville, VIC, Australia, with the University of California, Berkeley, CA, USA, with The University of Newcastle, with Lund University, Lund, Sweden, with the University of Munich, Munich, Germany, with the City University of Hong Kong, and with The Hong Kong Polytechnic University, Hong Kong. His research interests include control systems, complex networks, power systems, and stability analysis. His current work is mainly on control and planning of future energy networks and basic stability and control questions for dynamic networks.

Prof. Hill was an Australian Research Council Federation Fellow with the Australian National University during 2005–2010, and also a Chief Investigator and the Theme Leader (complex networks) with the ARC Centre of Excellence for Mathematics and Statistics of Complex Systems in 2006. He is a Fellow of the Society for Industrial and Applied Mathematics, Philadelphia, PA, USA, the Australian Academy of Science, Canberra, ACT, Australia, and the Australian Academy of Technological Sciences and Engineering, Melbourne, VIC, Australia. He is also a Foreign Member of the Royal Swedish Academy of Engineering Sciences.

Tao Liu (M'13) received the B.E. degree from Northeastern University, Shenyang, China, in 2003, and the Ph.D. degree from Australian National University, Canberra, ACT, Australia, in 2011.

From January 2012 to May 2012, he was a Research Fellow with the Research School of Engineering, Australian National University. During this period, he was also a Visiting Scholar with the Centre for Future Energy Networks, The University of Sydney, Sydney, NSW, Australia. From June 2012 to August 2013, he was a Postdoctoral Fellow with the University of Groningen, The Netherlands. In September 2013, he moved to The University of Hong Kong, Hong Kong, and was a Postdoctoral Fellow until June 2015. He is currently a Research Assistant Professor with the Department of Electrical and Electronic Engineering, The University of Hong Kong. His research interests include power systems, dynamical networks, distributed control, event-triggered control, and switched systems.